NASA TECHNICAL NOTE

NASA TN D-6149

NASA TN D-6149

EXPERIMENTAL BIAXIAL CREEP DATA FOR TANTALUM, MOLYBDENUM, AND ALLOYS T-111, TZM, AND TZC

by William L. Maag and William F. Mattson

Lewis Research Center
Cleveland, Ohio 44135

NATIONAL AERONAUTICS AND SPACE ADMINISTRATION • WASHINGTON, D. C. • FEBRUARY 1971

1. Report No. NASA TN D-6149	2. Government Accession No.	3. Recipient's Catalog No.
4. Title and Subtitle EXPERIMENTAL BIAXIAL CREEP DATA FOR TANTALUM, MOLYBDENUM, AND ALLOYS T-111, TZM, AND TZC		5. Report Date February 1971 6. Performing Organization Code
7. Author(s) William L. Maag and William F. Mattson		8. Performing Organization Report No. E-5822
9. Performing Organization Name and Address Lewis Research Center National Aeronautics and Space Administration Cleveland, Ohio 44135		10. Work Unit No. 120-27 11. Contract or Grant No.
12. Sponsoring Agency Name and Address National Aeronautics and Space Administration Washington, D.C. 20546		13. Type of Report and Period Covered Technical Note 14. Sponsoring Agency Code

15. Supplementary Notes

16. Abstract

This report presents experimental, biaxial steady-state creep data for tantalum, T-111, molybdenum, TZM, and TZC. The test conditions covered a temperature range of 1340 to 1922 K (1950° to 3000° F), a stress range of 2.76×10^{6} to 2.21×10^{8} N/m^{2} (400 to 32 000 psi), creep rates of 10^{-6} to 10^{-3} hr^{-1}, and durations of 100 to 1000 hours. The tests were conducted on internally pressurized thin-wall tubes. The biaxial creep data were analyzed using the von Mises criterion for plastic flow. The data, in terms of effective stresses and strain rates, were compared with uniaxial data of other investigators and the results were equivalent. Creep-rate correlations for each material are presented.

17. Key Words (Suggested by Author(s))	18. Distribution Statement
Biaxial creep Creep-rate correlations Tantalum Molybdenum Refractory alloys	Unclassified - unlimited

19. Security Classif. (of this report)	20. Security Classif. (of this page)	21. No. of Pages	22. Price*
Unclassified	Unclassified	26	$3.00

*For sale by the National Technical Information Service, Springfield, Virginia 22151

EXPERIMENTAL BIAXIAL CREEP DATA FOR TANTALUM, MOLYBDENUM, AND ALLOYS T-111, TZM, AND TZC

by William L. Maag and William F. Mattson

Lewis Research Center

SUMMARY

This report presents experimental, biaxial steady-state creep data for tantalum and its alloy T-111 and molybdenum and its alloys TZM and TZC. The test conditions included a temperature range of 1340 to 1922 K (1950° to 3000° F), a stress range of 2.76×10^6 to 2.21×10^8 N/m^2 (400 to 32 000 psi), creep rates of 10^{-3} to 10^{-6} hr^{-1}, and test durations of 100 to 1000 hours.

These refractories have application as cladding materials for high-temperature fuel pins used in liquid-metal-cooled nuclear reactors. The creep tests were conducted on internally pressurized thin-wall tubes to simulate the multiaxial stresses and strains in an operating fuel pin. The resulting biaxial creep data were analyzed using the von Mises criterion for plastic flow. These data, in terms of effective stresses and strain rates, were compared with uniaxial creep data of other investigators for the same materials at similar test conditions. The results showed that the biaxial and uniaxial creep properties of these refractories were equivalent when compared at the same effective stress and strain.

Steady-state creep-rate correlations were determined for each material for both the biaxial data and a combination of biaxial and uniaxial data. The correlating equation expressed the effective stress in terms of a power function and the temperature as an exponential function. Graphs are presented showing the experimental data in relation to each correlating equation.

INTRODUCTION

Refractory materials used in high-temperature designs are frequently subjected to multiaxial stresses that may result in multiaxial creep strains. Prediction of these strains is usually based on hypothetical relations between uniaxial creep and multiaxial

creep. Experimental data relating uniaxial and multiaxial creep are available for the more common materials such as lead, aluminum, and the steels. This study provides multiaxial creep data for five refractory metals and alloys and compares the results with uniaxial creep data for the same materials obtained by the conventional tensile creep test. The materials investigated are the refractory metal tantalum and its alloy T-111 (Ta-8W-2Hf) and molybdenum and its alloys TZM (Mo-0.5Ti-0.08Zr-0.03C) and TZC (Mo-1.2Ti-0.25Zr-0.15C). These materials have particular applications to space power nuclear reactors. As fuel-pin cladding material they are fabricable, possess good high-temperature strength and in proper combination are compatible with liquid metals and nuclear fuels.

The experimental model used herein to obtain multiaxial creep data was the internally pressurized thin-wall tube having diameter-to-wall-thickness ratios greater than 15. This model exhibits a biaxial creep condition in which the ratio of the two larger principal stresses (tangential and axial) is approximately 2 to 1 and the third principal stress is small and negative. This model was chosen because it approximates the multiaxial creep conditions of an operating fuel pin and because it offers a relatively simple theoretical relation between multiaxial and uniaxial creep when the von Mises criterion for plastic flow (refs. 1 and 2) is used.

The experimental biaxial creep data in the form of equivalent uniaxial stresses and strain rates were correlated by the method of reference 3, in which stress is expressed as a power function and temperature as an exponential function. These data were compared with conventional uniaxial creep data reported by various investigators (refs. 4 to 7) for similar test conditions. The experimental conditions include a temperature range of 1340 to 1922 K (1950° to 3000° F), a stress range of 2.76×10^{6} to 2.21×10^{8} N/m^{2} (400 to 32 000 psi), creep rates of 10^{-3} to 10^{-6} hr^{-1}, test times of 100 to 1000 hours, and similar chemical compositions and thermomechanical histories for the test specimens of each material.

APPARATUS AND PROCEDURE

The method of testing was to subject the test material to a multiaxial stress at a constant high temperature for a known period of time and to measure the resulting creep strain. The material was in the form of a tube. The multiaxial stress was applied by internally pressurizing the tube with argon gas. Temperature was controlled in a constant temperature furnace with an argon gas environment. Contamination of each test specimen was minimized by thorough cleaning procedures, wrapping each tube in a gettering foil and using high-purity argon gas for the test environment. Table I shows that the change in specimen compositions for randomly selected tubes was maintained at an acceptably low level by these precautions.

The multiaxial creep-rate data were converted to equivalent uniaxial data by the method of reference 2, correlated by the method of reference 3, and compared with existing uniaxial creep-rate data for the same materials and similar test conditions.

Test Specimen

Figure 1 is a sketch of a typical test specimen. The tubes were drilled and lapped using both extruded tube stock and bar stock. Caps of the same material were welded to both ends. A small-diameter pressurizing tube of either tantalum or molybdenum, depending on the specimen material, was welded into one end cap. The tube specimen was either 6.35 or 7.62 centimeters (2.5 or 3 in.) long and 1.59±0.00254 centimeters (0.625±0.001 in.) in outside diameter. Wall thickness was either 0.0254±0.00127 centimeter (0.010±0.0005 in.), 0.0508±0.00254 centimeter (0.020±0.001 in.) or 0.1016±0.00254 centimeter (0.040±0.001 in.). The pressurizing tube was 0.3175 centimeter (0.125 in.) in outside diameter, 0.0635 centimeter (0.025 in.) in wall thickness, and 30.48 centimeters (12 in.) long. The inside and outside surface finish for the tube specimen was 64 rms or better. The parts for each tube assembly were inspected for dimensional tolerance and surface imperfections and then degreased in acetone and alcohol before welding. All welding was done by the electron-beam method in a vacuum of 10^{-6} torr or by the gas tungsten-arc method in an argon-purged dry box. Each completed specimen was leak tested using a helium mass spectrometer detector to ensure the integrity of all welds. An identifying symbol was scribed on the bottom cap of each tube specimen with a vibrating pencil.

Test Apparatus

The test apparatus is shown schematically in figure 2, and the test facility in figure 3. It consisted of a high-temperature furnace in which the tube specimens were positioned. Each tube was connected to a high-pressure gas system via the small pressurizing tube. Instruments for measuring pressure and temperature were provided. Two identical set of equipment were used for these tests. Each had a capacity to test 30 tube specimens at a time, but a typical load was about 10 tubes.

Each tube specimen was cleaned in alcohol and wrapped in 0.0025-centimeter-(1-mil-) thick tungsten foil. All tubes for each run were positioned in a molybdenum can which was then packed with tungsten wool. The purpose of these steps was to minimize the chemical reaction of the specimen material with any environmental contaminants such as hydrocarbons or oxygen and nitrogen. A measure of the success of this effort is shown in table I, which reports the increase in contaminant content for representative

test specimens. The small increases in contamination indicate that this effect was not a significant factor in the creep results reported herein.

This method of packing also eliminated a vibration problem that occurred when the specimens were suspended individually inside the furnace. The tubes and the molybdenum can were suspended from the furnace cover plate through 0.3175-centimeter-(0.125-in.-) diameter packing glands. After the furnace cover was in place, the small pressurizing tubes were individually connected to the gas pressurization system.

The purging procedure was as follows: (1) the furnace was evacuated with a mechanical vacuum pump to a vacuum of 10^{-2} torr and then filled with argon to a pressure of 1.22×10^{5} N/m^2 (3 psig), (2) the tube specimens were internally pressurized to 7.92×10^{5} N/m^2 (100 psig) with argon and exhausted to the atmosphere, and (3) both purging operations were repeated five times. The result was a contaminant concentration equal to the purity of the argon gas, which was a high purity grade whose oxygen content was less than 1 ppm.

The next step was to set the furnace pressure at slightly above atmospheric, power the furnace to the desired temperature, and pressurize each tube to produce a predetermined stress. The test temperature was determined with a micro-optical pyrometer sighting through a viewing port onto a blackbody suspended in the furnace hot zone. The maximum furnace temperature was 2273 K (3632° F). The temperature was maintained within ±2 K by controlling the heater power input. Thermocouples were used initially to monitor temperature but the stability of the power controller proved them unnecessary. The temperature gradient along the length of the tube specimen was less than 3 K.

The maximum rating for the pressurizing system was 8.36×10^{6} N/m^2 (1200 psig). A precision pressure gage with a range of 0 to 1.39×10^{7} N/m^2 (0 to 2000 psig) and accurate to $\pm6.89\times10^{3}$ N/m^2 (1 psi) was used to measure the pressure in each tube. Once the tube was pressurized, the pressure was sealed in the tube by closing a valve. Leakage from the closed system was practically nil for the duration of the test. However, since the room temperature was not constant and a significant portion of the gas system was at room temperature, the tube pressure could vary as much as ±1 percent during the test period. For the first few tubes tested, the tube pressure was monitored with pressure transducers but the stability of the pressure reading proved this unnecessary for subsequent tests.

Material

The material tested was procured from commercial vendors in the form of bar stock or seamless tubing. The original form for each material was an arc-melted ingot that was extruded to a 1.905 centimeter (0.75 in.) diameter bar or tube. This

material was recrystallized prior to machining into the final test tube dimensions. The chemical compositions of representative heats tested are given in table II. After machining and assembly into a test specimen, each tube received a 1-hour heat treatment at 1922 K (3000° F) before pressurization and testing commenced.

Measurements

The tangential creep rate was determined by measuring the outside diameter of the tube before and after each test and dividing the difference by the time at temperature and stress. No correction for true strain was used. The measurements were made at room temperature on the unpressurized tube, thereby excluding the elastic and thermal expansion components of strain. However, any primary creep that may have occurred was included. Primary creep may have been a significant factor for the pure metal tantalum and possibly molybdenum but was not considered significant for the refractory alloys T-111, TZM, and TZC for the following reasons:

(1) Continuous uniaxial creep curves for these refractory alloys (ref. 4) indicated the amount of primary creep strain was usually less than 0.1 percent at similar test conditions. Most of the total strains for this investigation were from 1 to 10 percent.

(2) Several tests were conducted with T-111 and TZM tubes for which the creep rate was determined after about 400 hours and again after about 800 hours at the same test conditions. The intermediate creep rates which should more closely represent steady-state creep differed from the total creep rates by less than 10 percent.

The outside tube diameter is an average of several measurements made at various locations along the tube with a micrometer with a least count of 0.000254 centimeter (0.0001 in.). To avoid end effects, the distance representing one length-diameter ratio (L/D) from each end was not included in the measurements. For strains less than about 10 percent, all measurements regardless of location were nearly identical, indicating little or no end effects. However, when the strains exceeded about 10 percent, the tube shape became more barrel-like and the diameter represented an average of several very different measurements.

The multiaxial stress and strain analysis described in the section Analysis used the creep rate based on the mean tube diameter, whereas the actual measurements represent the outside tube diameter. The mean creep rate was calculated from the test measurements by the following approximation:

$$\dot{\epsilon}_m = \frac{\dot{\epsilon}_o}{2}\left(1 + \frac{D_o^2}{D_i^2}\right)$$

which was derived using the assumption of constant volume. For the three differing-wall-thickness tubes tested, this correction factor was 1.14, 1.07, and 1.03, respectively. The second correction factor $(2/\sqrt{3})$, which converts the mean tangential creep rate to an effective uniaxial creep rate, is described in the Analysis section.

Analysis

The state of stress in a material at a constant temperature is defined by the three principal stresses. The conditions at which plastic flow occurs for multiaxial stresses can be predicted with reasonable accuracy by the von Mises flow criterion. The von Mises equations that define the states of stress and strain rates for an isotropic material are

$$\sigma_{eff} = \frac{1}{\sqrt{2}} \sqrt{(\sigma_1 - \sigma_2)^2 + (\sigma_2 - \sigma_3)^2 + (\sigma_3 - \sigma_1)^2} \tag{1}$$

$$\dot{\epsilon}_{eff} = \frac{\sqrt{2}}{3} \sqrt{(\dot{\epsilon}_1 - \dot{\epsilon}_2)^2 + (\dot{\epsilon}_2 - \dot{\epsilon}_3)^2 + (\dot{\epsilon}_3 - \dot{\epsilon}_1)^2} \tag{2}$$

Soderberg (ref. 2) presented an equation for each principal creep rate in terms of the effective stress, the effective creep rate, and the principal stress as follows:

$$\dot{\epsilon}_1 = \frac{\dot{\epsilon}_{eff}}{\sigma_{eff}} \left[\sigma_1 - \frac{1}{2}(\sigma_2 + \sigma_3)\right] \tag{3}$$

$$\dot{\epsilon}_2 = \frac{\dot{\epsilon}_{eff}}{\sigma_{eff}} \left[\sigma_2 - \frac{1}{2}(\sigma_3 + \sigma_1)\right] \tag{4}$$

$$\dot{\epsilon}_3 = \frac{\dot{\epsilon}_{eff}}{\sigma_{eff}} \left[\sigma_3 - \frac{1}{2}(\sigma_1 + \sigma_2)\right] \tag{5}$$

For the case of uniaxial creep, $\sigma_2 = \sigma_3 = 0$. Substituting these values into equations (1) and (3) shows that the effective stress and creep rate are equal to the principal uniaxial stress σ_1 and principal uniaxial creep rate $\dot{\epsilon}_1$, respectively.

The state of stress for an internally pressurized thin-wall tube may be defined by the three principal stresses acting in the tangential, radial, and axial directions. For a thin-wall tube, these stresses are defined as

$$\sigma_1 = \sigma_t = \frac{PD_m}{2w} - \frac{P}{2}$$

$$\sigma_2 = \sigma_r = -\frac{P}{2}$$

$$\sigma_3 = \sigma_a = \frac{PD_m}{4w} - \frac{P}{2}$$

The radial stress $-P/2$ is small relative to the other stresses for this study. Solving equations (1), (3), (4), and (5) in terms of the tangential stress gives

$$\sigma_{eff} = \frac{\sqrt{3}}{2}\sigma_t$$

$$\dot{\epsilon}_{eff} = \frac{2}{\sqrt{3}}\dot{\epsilon}_t$$

In terms of the principal creep rates,

$$\dot{\epsilon}_t = \frac{\sqrt{3}}{2}\dot{\epsilon}_{eff}$$

$$\dot{\epsilon}_r = -\dot{\epsilon}_t$$

$$\dot{\epsilon}_a = 0$$

These relations state that a uniaxial creep test and an internally pressurized tube creep test, conducted at the same temperature with the same material, will result in equal effective stresses and strains if the thin-wall tube is pressurized to a tangential stress that is $2/\sqrt{3}$ times that of the uniaxial stress in a tensile specimen. The result-

ing tangential creep rate will be $\sqrt{3}/2$ times that of the uniaxial creep rate and the walls will thin at that same rate. The tube length will remain constant.

Both the biaxial creep data of this investigation and the uniaxial creep data of other investigators were correlated by the statistical method presented in reference 3. The empirical equation used for high-temperature, steady-state creep rate is

$$\dot{\epsilon} = A\sigma^n \exp\left(\frac{-\Delta H}{RT}\right) \tag{6}$$

where A is a constant that includes such structural effects as grain size, dislocation density, and other microstructural features; n is the stress exponent that normally has a value of about 5 for pure metals and about 3 for alloys; and ΔH is the activation energy for the controlling creep mechanism, which at high temperatures is similar to the energy required for self-diffusion.

RESULTS AND DISCUSSION

The effective biaxial creep rate data of this investigation are presented in table III. The data include the following range of test conditions and results:

Temperature, K (°F)	1340 to 1922 (1950 to 3000)
Effective stress, N/m^2 (psi)	2.76×10^6 to 2.21×10^8 (400 to 32 000)
Effective creep rate, hr^{-1}	10^{-3} to 10^{-6}
Diametral strain, percent	0.1 to 30
Test duration, hr	100 to 1000

The effective biaxial data for each material are presented graphically in figures 4(a) to 8(a). The curves on semi-log plots represent the straight-line equation

$$\frac{\dot{\epsilon}}{\sigma^n} = A \exp\left(-\frac{\Delta H}{RT}\right) \tag{7a}$$

or

$$\log \frac{\dot{\epsilon}}{\sigma^n} = \log A - \frac{\Delta H}{2.303\ R}\left(\frac{1}{T}\right) \tag{7b}$$

which are rearrangements of equation (6) that permit showing the effects of three variables on a two-dimensional plot. The constants n, A, and ΔH were determined from a least-squares analysis of the experimental data (ref. 3). The data points represent the experimental values of temperature, effective stress, and effective creep rate. The dashed lines are located ± 1 standard deviation from the correlating line and form a region within which approximately two-thirds of the experimental data fall; they thereby provide a measure of data scatter and reliability of the correlation equation. This variation for each correlation is presented in table IV.

Figures 4(b) to 8(b) show the correlation resulting from combining the effective biaxial creep data of this investigation with uniaxial creep data obtained by other investigators for the same material tested at similar conditions. These figures thus give a direct comparison between the biaxial and uniaxial creep properties of the material.

The empirical equations for both biaxial and combined data, presented in figures 4 to 8, generally represent the experimental creep-rate data within plus and minus a factor of 5, which is reasonably good agreement for predicting refractory-metal creep rate. The use of equation (6) to characterize high-temperature creep properties implies that the energy term, ΔH, is analogous to the activation energy for self-diffusion and that the exponent for the stress function should agree with the accepted values of 4 to 6 for pure metals and 2 to 4 for alloys (ref. 8). This, in fact, was the result for most of the materials tested. Table IV compares the empirical constants with the ideal values.

The biaxial test results for the pure metal tantalum were the poorest of the materials tested. One reason for this may be because tantalum exhibits an appreciable amount of primary creep which was not considered by this investigation. The combination of biaxial and uniaxial data represents a better correlation as evidenced by the closer agreement between the ideal and empirical correlation constants shown in table IV.

The biaxial creep properties of T-111 were of particular interest because this tantalum alloy is being considered as a fuel-element cladding material for space power nuclear reactors. The correlation for the biaxial data represents the majority of the creep rate data within a factor of ± 1.5. These data included three heats of materials and both extruded and bored tube specimens. The combined biaxial and uniaxial correlation represents the majority of the data within a factor of ± 1.8. Included in these data are eight different heats of material. All the T-111 biaxial and uniaxial data represent a heat treatment of 1 hour at 1922 K (3000° F) prior to creep testing. The good agreement of the energy and stress constants with each other and with the ideal values shown in table IV attests to the similarity and quality of these correlations. Photomicrographs of representative, biaxially creep-tested T-111 specimens are shown in figure 9. The effect of test temperature on grain size is apparent.

The molybdenum biaxial data correlated satisfactorily, and primary creep did not appear to be a significant factor. The fact that the strains for the molybdenum materials were generally much greater than for the tantalum materials would tend to minimize the effect of the primary portion of the creep curve. The combination of uniaxial and biaxial data actually resulted in a poorer correlation for molybdenum, both from the standpoint of variability and agreement between correlation constants. Reasons for this would include different heat treatments and much higher carbon contents (140 and 250 ppm) for the uniaxial materials.

The biaxial and combined biaxial and uniaxial correlations for the molybdenum alloy TZM were both satisfactory. Stress and energy constants for both equations agreed very closely with the ideal values of table IV. The biaxial correlation of figure 7(a) represents only one heat of material, whose composition is given in table II, and a 1-hour heat treatment at 1922 K (3000° F) before creep testing. The combined correlation of figure 7(b) represents two heats of material and two heat treatments with the uniaxial specimens being heat treated 1 hour at 1700 K (2200° F) before creep testing.

The biaxial data for the molybdenum alloy TZC correlated satisfactorily, as shown in figure 8(a). However, the correlation constants were not in agreement with the ideal values of table IV. The combination of biaxial and uniaxial data, shown in figure 8(b), resulted in a poorer correlation. The combination represents two heats of material but both received the same heat treatment of 1 hour at 1922 K (3000° F) prior to creep testing. The reason for this apparent nonconformity of the biaxial and uniaxial creep properties of TZC is not known.

The chief significance of figures 4 to 8 is the reasonably good agreement that exists between effective biaxial and uniaxial creep data for these refractory metals and alloys. The equations representing these data may be used for design purposes if the variability and test conditions associated with each are fully recognized. The combined correlations better represent the materials simply because a greater variety of data was used to determine them.

Representative creep-tested tube specimens are shown in figure 10. The tantalum and T-111 tubes were seldom strained more than about 5 percent because of problems with the pressurizing tubes, so the change in diameter is not obvious in the photograph. Strains for the molybdenum and molybdenum alloy tubes were generally much greater, with many specimens tested to incipient failure or failure. This is evidenced by the roughened, shiny skin and the development of longitudinal cracks in these tubes. Most failures occurred gradually and were evidenced by a gradual loss of gas pressure over a period of several hours. However, a few tubes ruptured suddenly as pictured by the T-111 specimen in figure 10.

SUMMARY OF RESULTS

An experimental study of the high-temperature, biaxial, steady-state creep properties of tantalum and its alloy T-111 and molybdenum and its alloys TZM and TZC was conducted using internally pressurized tube specimens. The test conditions included a temperature range of 1340 to 1922 K (1950° to 3000° F), a stress range of 2.76×10^6 to 2.21×10^8 N/m^2 (400 to 32 000 psi), and creep rates of 10^{-3} to 10^{-6} hr^{-1}. The results were

1. The biaxial and uniaxial creep properties of these refractory metals and alloys are equivalent when compared on the basis of effective stress and strain rate as defined by the von Mises criterion for plastic flow.

2. Steady-state creep-rate correlations were determined for each material for both the biaxial data and a combination of biaxial and uniaxial data. The correlations for T-111, molybdenum, and TZM represented the experimental data very closely, and the correlation constants agreed with generally accepted values from other investigators. The tantalum correlations were not too satisfactory probably because the biaxial data included a significant amount of primary creep. The TZC correlation adequately represented the biaxial data but the combined biaxial and uniaxial data resulted in a relatively poor correlation.

3. For design purposes the correlations that combine the effective biaxial and uniaxial data better represent the materials because they include a greater variety of data and hence a more representative sample.

Lewis Research Center,
National Aeronautics and Space Administration,
Cleveland, Ohio, October 15, 1970,
120-27.

APPENDIX - SYMBOLS

A	constant, $hr^{-1} (Nm^{-2})^{-n}$
D	diameter, cm
ΔH	activation energy, J/g-mole
n	stress-dependency constant
P	internal pressure, N/m^2
R	gas constant, 8.3143 J/(g-mole)(K)
T	absolute temperature, K
w	wall thickness, cm
$\dot{\epsilon}$	creep rate, hr^{-1}
σ	stress, N/m^2

Subscripts:

a	axial
eff	effective
i	inside
m	mean
o	outside
r	radial
t	tangential

REFERENCES

1. Manson, S. S.: Thermal Stress and Low-Cycle Fatigue. McGraw-Hill Book Co., Inc., 1966, p. 89.

2. Soderberg, C. R.: Interpretation of Creep Tests on Tubes. Trans. ASME, vol. 63, no. 8, Nov. 1941, pp. 737-748.

3. Maag, William L.; and Mattson, William F.: Statistical Analysis of High-Temperature Creep-Rate Data for Alloys of Tantalum, Molybdenum, and Columbium. NASA TN D-5424, 1969.

4. Sawyer, J. C.; and Steigerwald, E. A.: Generation of Long Time Creep Data of Refractory Alloys at Elevated Temperatures. NASA CR-1115, 1968.

5. Sawyer, J. C.; and Sheffler, K. D.: Generation of Long Time Creep Data on Refractory Alloys at Elevated Temperatures. TRW Equipment Labs. (NASA CR-72319), Aug. 1, 1967.

6. Stephenson, R. L.: Creep-Rupture Properties of Unalloyed Tantalum, Ta-10%W and T-111 Alloys. Rep. ORNL-TM-1994, Oak Ridge National Lab., Dec. 1967.

7. Anon.: AEC Fuels and Materials Development Program Annual Report January 31, 1967 - January 31, 1968. Rep. GEMP-1004, General Electric Co., Mar. 31, 1968, pp. 45-46.

8. Garofalo, Frank: Fundamentals of Creep and Creep-Rupture in Metals. Macmillian Co., 1965.

TABLE I. - CONTAMINANT CHANGE DURING TESTING

Material	Wall thickness, cm	Oxygen	Carbon	Hydrogen	Nitrogen
		Chemical composition change, ppm			
Tantalum	0.0254	+270	-20	---	+46
	.0508	+120	+3	---	+36
	.1016	+105	-21	+16	+51
T-111	0.0254	+91	+19	---	-4
	.0254	+111	+14	---	+2
	.0508	+35	+8	+10	-6
	.1016	+4	-6	-5	-6
	.1016	+1	-6	+1	+4
	.1016	+7	-1	+4	-1

TABLE II. - CHEMICAL COMPOSITION OF SPECIMEN MATERIAL

Element	Tantalum	T-111	Molybdenum	TZM	TZC
			Composition in ppm unless noted		
Al	<5	<10			
B	<5				
C	35	25	10	0.014 wt. %	0.11 wt. %
Ca	5				
Cb	35	350			
Co	(a)	<5			
Cr	<5	<10			
Cu	<5	<20			
Fe	<5	20	<10	<20	
H	1	2	1	1	
Hf		2.0 wt. %			
Mg	<5				
Mn	<5				
Mo	<5	15	Balance	Balance	Balance
N	<10	12	1	3	
Ni	<5	<10	<10	<10	
O	<50	45	<5	13	
Si	<5	<20	<10	<20	
Sn	(a)				
Ta	Balance	Balance			
Ti	<5	<20		0.49 wt. %	1.19 wt. %
V		<10			
W	(a)	7.95 wt. %			
Zr	<5			0.088 wt. %	0.17 wt. %
Hardness (DPH)	-------	207 to 217	233 to 238	279 to 287	285 to 292

[a]None detected.

TABLE III. - EXPERIMENTAL BIAXIAL TEST RESULTS

Material	Temperature, K	Effective stress, N/m^2	Effective steady-state creep rate, hr^{-1}	Diametral strain, percent	Wall thickness, cm
Tantalum	1367	2.75×10^{7}	8.88×10^{-5}	0.9	0.0254
	1367	3.62	3.30×10^{-4}	3.2	.0381
	1644	1.21	5.51	3.4	.0381
	1922	2.62×10^{6}	7.81×10^{-5}	2.3	.1016
	1810	4.34	5.69	1.7	.1016
	1810	3.48	3.98	1.2	.1016
	1478	9.65	2.61	.4	.0381
	1478	2.20×10^{7}	2.01×10^{-4}	3.2	.0254
	1588	9.72×10^{6}	3.08×10^{-5}	.5	.0381
	1588	9.03	2.11	.7	.0508
	1699	7.24	4.45	3.1	.0508
T-111	1588	5.47×10^{7}	5.00×10^{-5}	1.4	0.0254
	1588	6.03	6.98	1.6	.0508
	1588	2.94	1.12	.3	.0508
	1810	1.83	7.84	2.2	.1016
	1810	1.49	5.67	1.7	.0508
	1810	1.51	4.60	1.3	.1016
	1699	3.00	6.06	.8	.1016
	1478	1.01×10^{8}	1.12×10^{-4}	1.6	.0254
	1367	1.10	1.52×10^{-5}	.5	.0254
	1367	1.43	1.36	.4	.0254
	1922	8.76×10^{6}	3.68	1.1	.1016
	1922	9.86	7.37	2.2	.0508
	1478	6.14	4.99×10^{-6}	.1	.0508
	1588	5.16×10^{7}	1.02×10^{-4}	3.3	.0254
	1478	8.12	1.44×10^{-5}	.2	.0508
	1699	2.83	8.85	1.3	↓
	↓	2.38	5.94	1.6	
		3.26	1.13×10^{-4}	2.7	
		2.32	4.60×10^{-5}	3.2	
	1810	2.72	5.71×10^{-4}	1.2	
	1810	1.54	4.54×10^{-5}	2.3	
	1810	1.61	5.43	2.6	
	1922	1.58	1.77×10^{-4}	5.0	↓
	1922	1.54	2.23	1.2	.1016
	1922	1.55	2.60	4.1	.1016
	1340	2.21×10^{8}	1.40×10^{-5}	.2	.0254
	1644	4.09×10^{7}	8.46	2.9	.0508
	1644	4.13	9.58	1.3	.1016

TABLE III. - Concluded. EXPERIMENTAL BIAXIAL TEST RESULTS

Material	Temperature, K	Effective stress, N/m^2	Effective steady-state creep rate, hr^{-1}	Diametral strain, percent	Wall thickness, cm
Molybdenum	1644	1.81×10^{7}	2.95×10^{-3}	20.0	0.0508
	1922	6.52×10^{6}	3.57	24.8	.1016
	1922	4.34	4.81×10^{-4}	14.2	.1016
	1810	6.55	3.38	9.8	.1016
	1810	6.79	1.55	4.5	.0508
	1588	1.17×10^{7}	8.50×10^{-5}	2.8	.0508
	1478	3.66	2.33×10^{-3}	6.7	.0254
	1699	6.96×10^{6}	7.76×10^{-5}	5.5	.1016
TZM	1367	1.10×10^{8}	4.87×10^{-6}	0.1	0.0254
	1922	1.75×10^{7}	3.98×10^{-3}	27.7	.1016
	↓	1.31	1.00	6.9	.1016
		1.12	9.07×10^{-4}	6.3	.0508
		8.72×10^{6}	8.52	8.0	.1016
	1810	1.75×10^{7}	3.32	6.8	.1016
	1588	5.58	2.01	6.4	.0254
	1588	4.58	1.84	6.0	.0254
	1478	1.10×10^{8}	7.02×10^{-5}	1.9	.0254
	1699	2.71×10^{7}	2.72×10^{-4}	7.3	.0508
	1699	2.71	3.38	20.0	.0508
	1810	8.72×10^{6}	5.27×10^{-5}	3.8	.1016
	↓	8.72	5.91	4.2	.1016
		1.14×10^{7}	7.77	5.5	.1016
		8.76×10^{6}	5.74	4.1	.0508
	1644	4.07×10^{7}	1.54×10^{-4}	5.4	.0508
TZC	1367	1.47×10^{8}	2.68×10^{-5}	0.7	0.0254
	1588	7.28×10^{7}	2.72×10^{-3}	18.4	.0508
	1588	9.19	3.80	9.9	.0254
	1478	1.47×10^{8}	3.07	6.1	.0254
	1478	1.10	1.36	12.4	.0254
	1810	2.71×10^{7}	1.66	15.1	.0508
	1699	3.43	1.29	15.7	.0508
	1699	3.25	1.07	12.4	.0508
	1922	1.26	7.80×10^{-4}	19.7	.1016
	1644	4.07	8.69	13.2	.0508

TABLE IV. - COMPARISON OF CORRELATION

VARIABILITY AND CONSTANTS

	Tantalum	T-111	Molybdenum	TZM	TZC
Variation for one standard deviation, $\dot{\epsilon}_{max}/\dot{\epsilon}$:					
Biaxial	2.1	1.5	1.8	1.5	1.8
Combined	2.1	1.8	1.9	2.0	4.2
Stress exponent, n:					
Ideal (ref. 8)	4 to 6	2 to 4	4 to 6	2 to 4	2 to 4
Biaxial	3.1	3.0	5.3	3.0	4.7
Combined	4.7	2.7	4.5	3.1	5.1
Activation energy, ΔH, kJ/g-mole:					
Ideal (ref. 8)	460	460	502	502	502
Biaxial	248	378	501	481	557
Combined	364	345	327	509	704

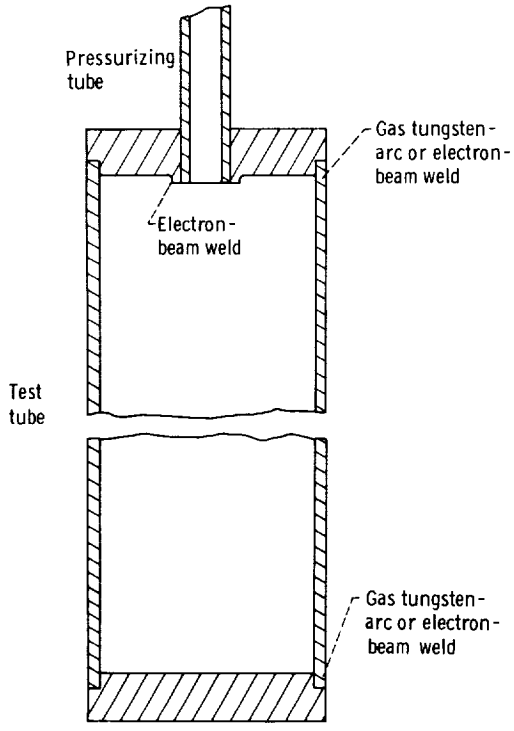

Figure 1. - Test specimen.

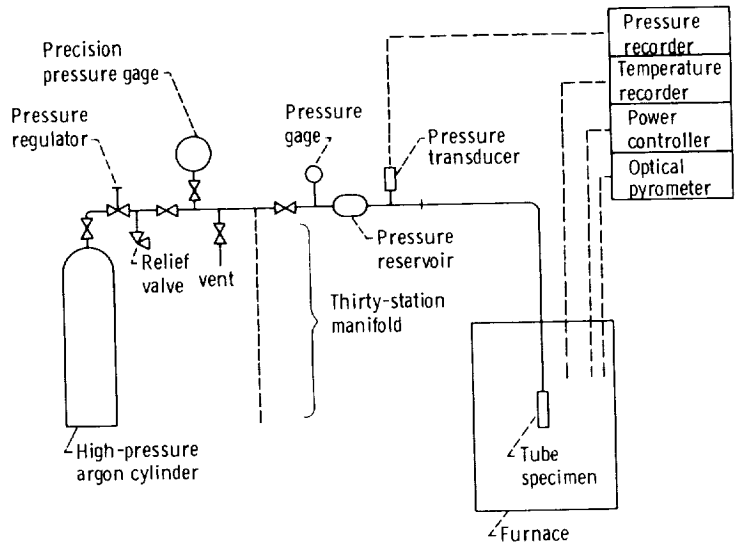

Figure 2. - Schematic of test apparatus.

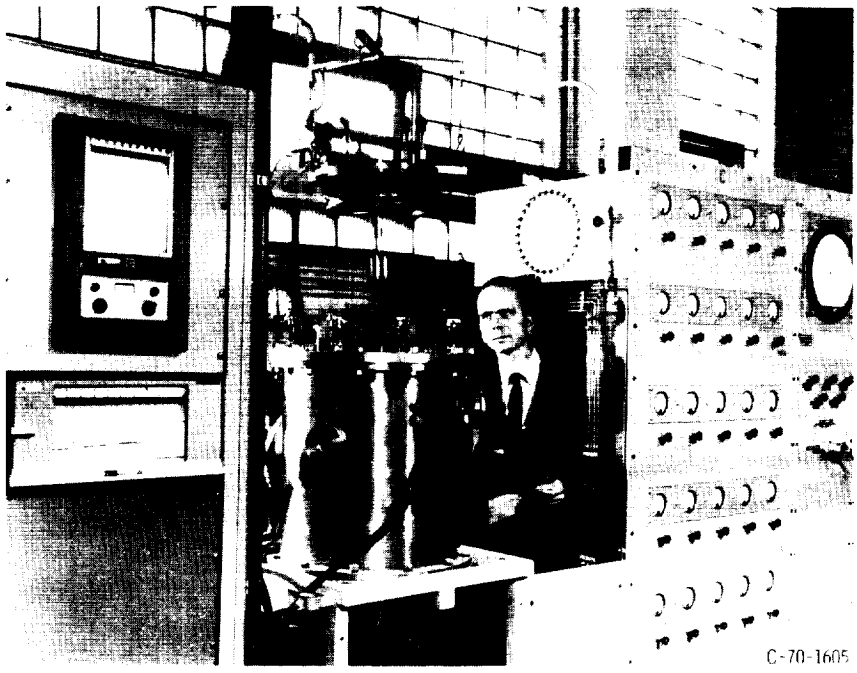

Figure 3. - Test facility.

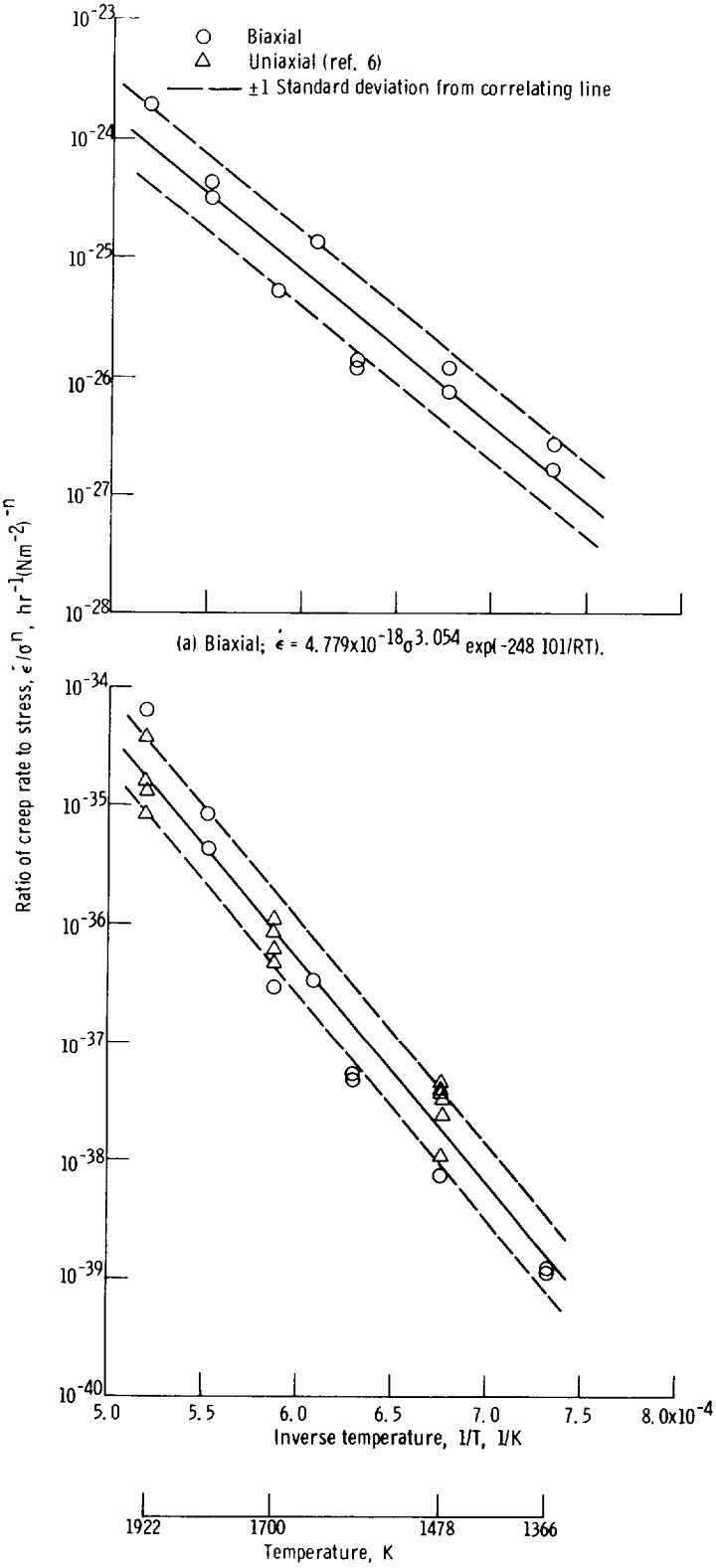

(a) Biaxial; $\dot{\epsilon} = 4.779 \times 10^{-18} \sigma^{3.054} \exp(-248\,101/RT)$.

(b) Uniaxial and biaxial; $\dot{\epsilon} = 1.356 \times 10^{-25} \sigma^{4.691} \exp(-364\,064/RT)$.

Figure 4. - Creep test results for tantalum.

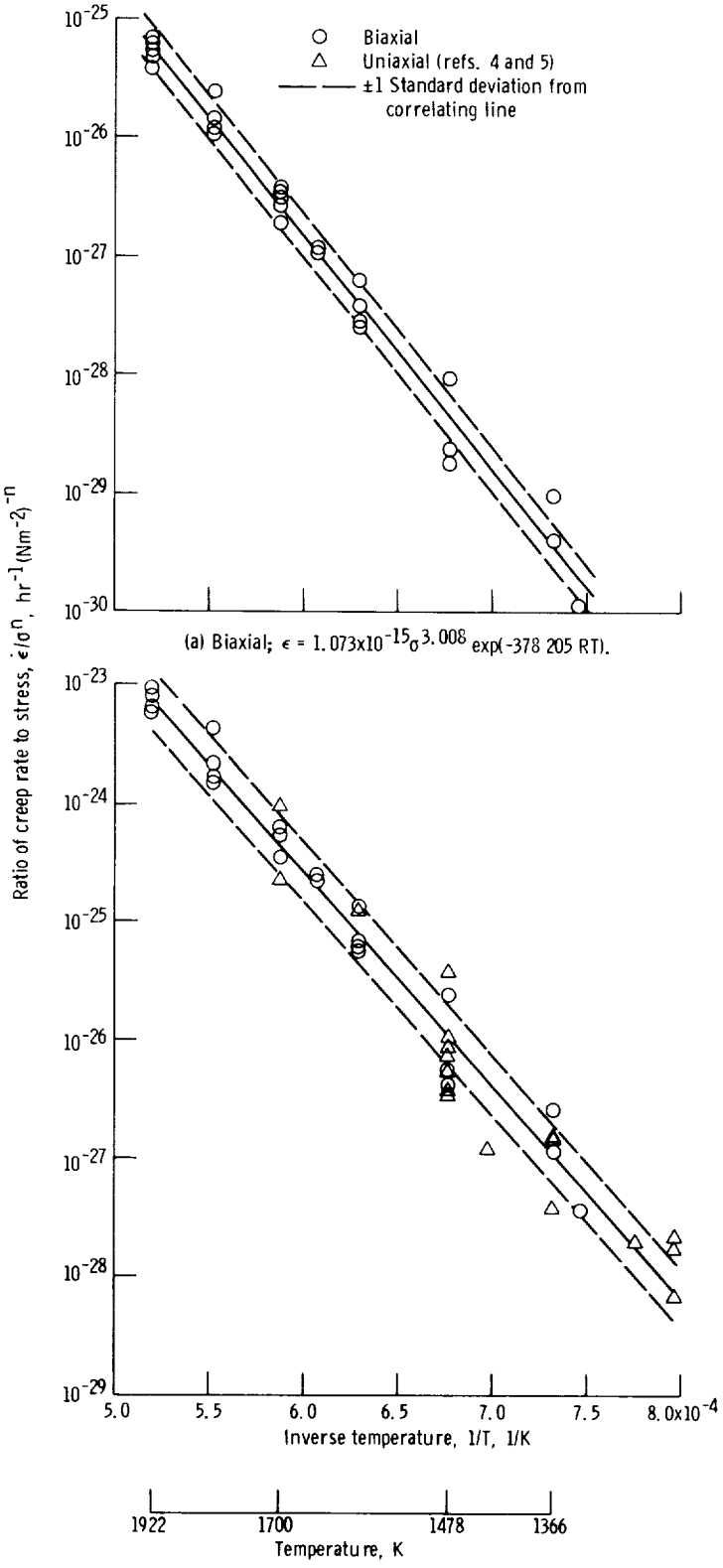

(a) Biaxial; $\dot{\epsilon} = 1.073 \times 10^{-15} \sigma^{3.008} \exp(-378\,205/RT)$.

(b) Uniaxial and biaxial; $\dot{\epsilon} = 1.755 \times 10^{-14} \sigma^{2.706} \exp(-345\,215/RT)$.

Figure 5. - Creep test results for T-111.

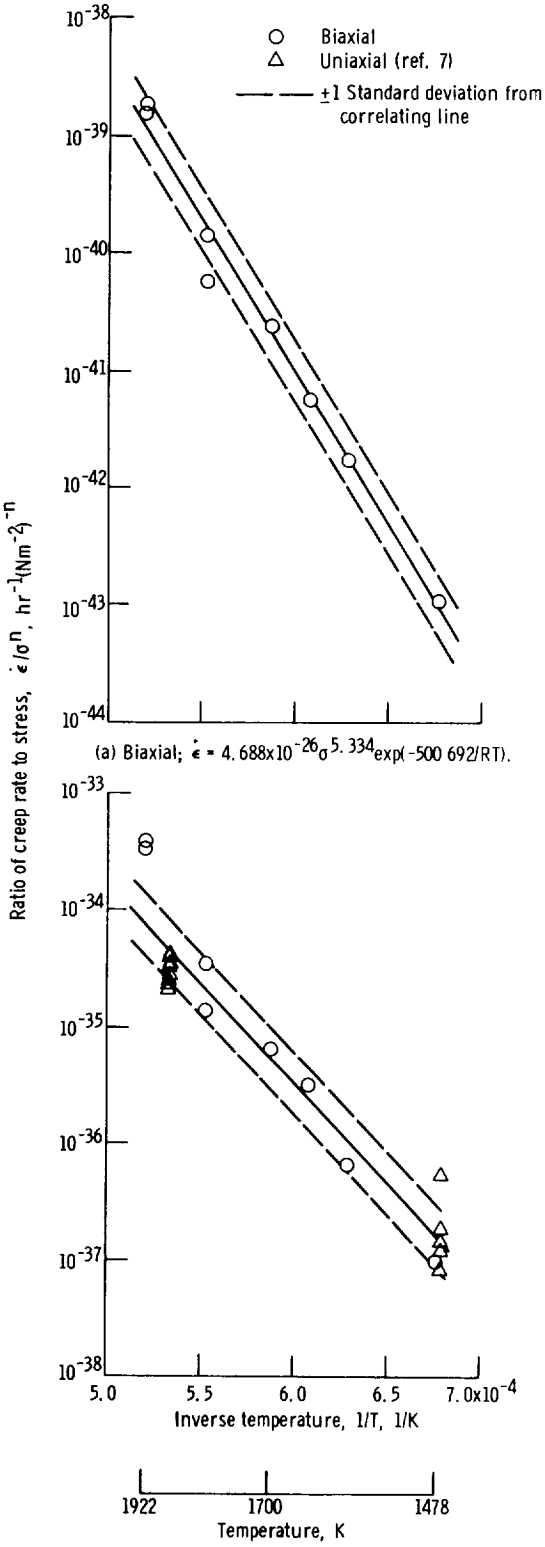

(a) Biaxial; $\dot{\epsilon} = 4.688 \times 10^{-26} \sigma^{5.334} \exp(-500\,692/RT)$.

(b) Uniaxial and biaxial; $\dot{\epsilon} = 6.061 \times 10^{-26} \sigma^{4.544} \times \exp(-327\,478/RT)$.

Figure 6. - Creep test results for molybdenum.

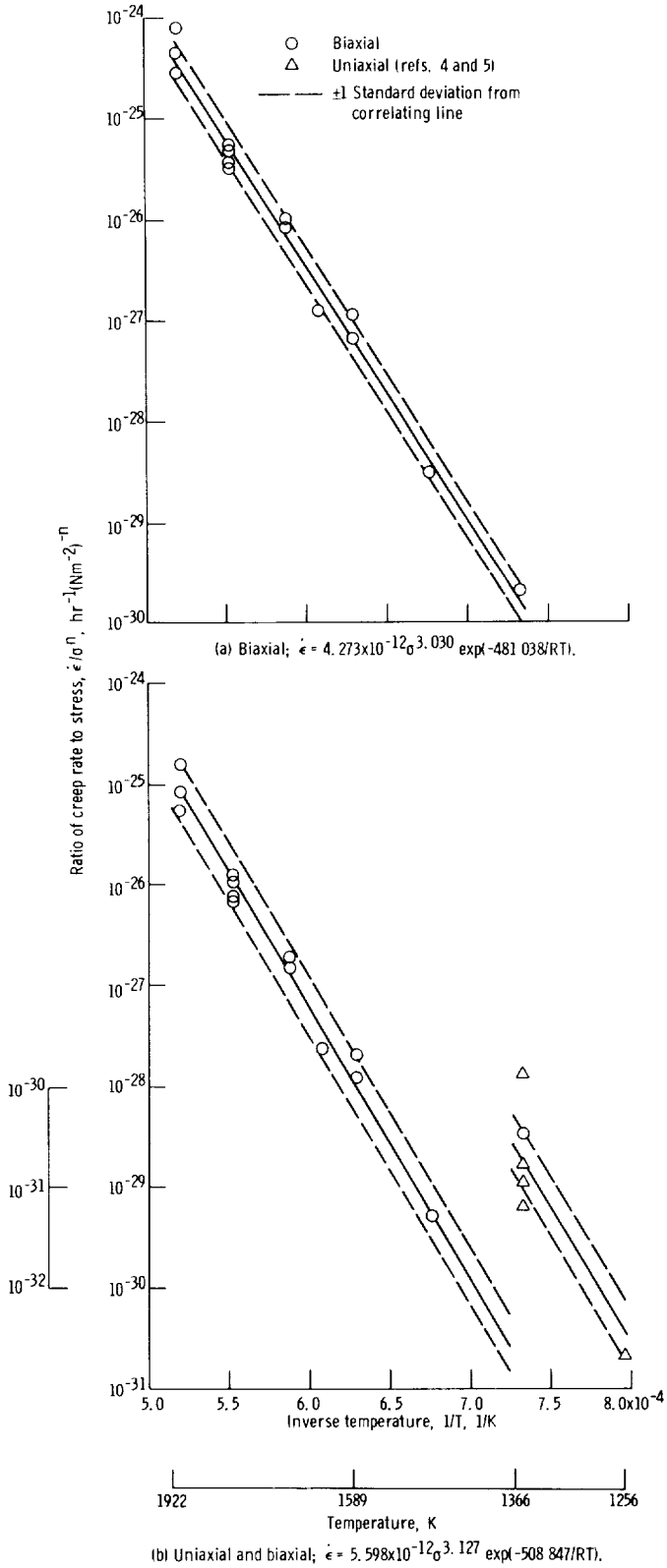

(a) Biaxial; $\dot{\epsilon} = 4.273 \times 10^{-12} \sigma^{3.030} \exp(-481\,038/RT)$.

(b) Uniaxial and biaxial; $\dot{\epsilon} = 5.598 \times 10^{-12} \sigma^{3.127} \exp(-508\,847/RT)$.

Figure 7. - Creep test results for TZM.

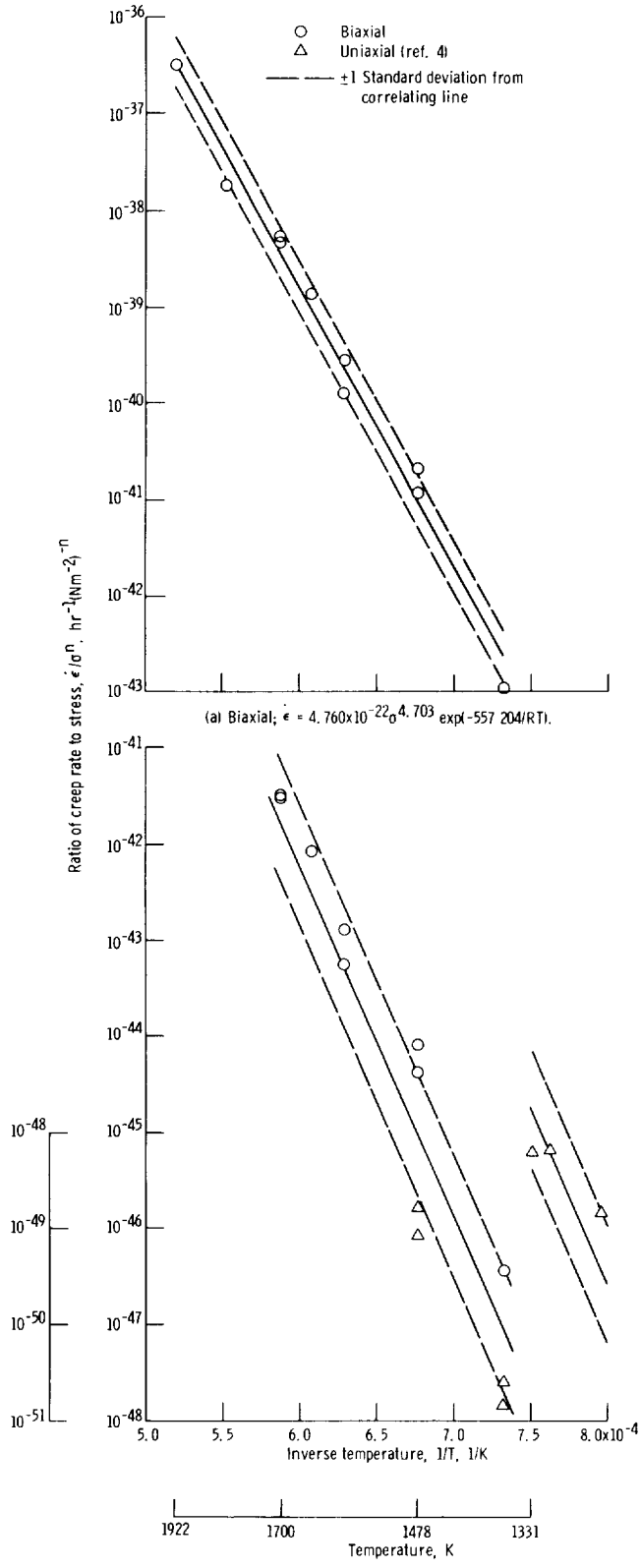

(a) Biaxial; $\dot{\epsilon} = 4.760 \times 10^{-22} \sigma^{4.703} \exp(-557\,204/RT)$.

(b) Uniaxial and biaxial; $\dot{\epsilon} = 7.282 \times 10^{-21} \sigma^{5.127} \exp(-703\,987/RT)$.

Figure 8. - Creep test results for TZC.

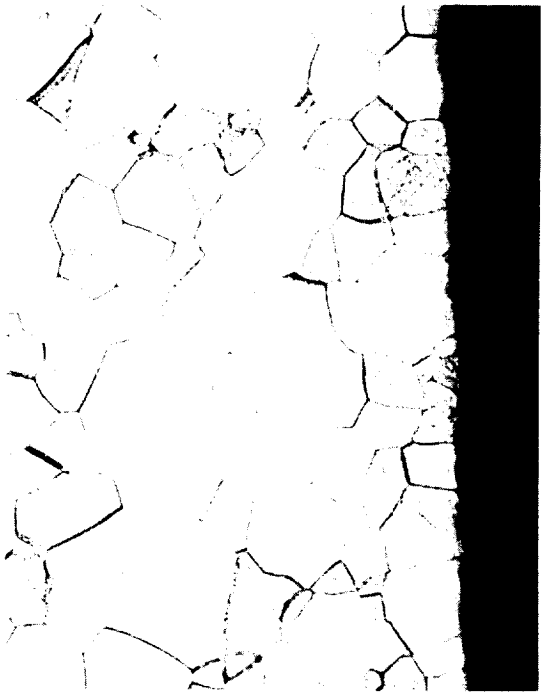

(a) After biaxial creep testing for 200 hours at 1478K (2200° F) and $6.14X10^6$ N/m^2 (8910 psi).

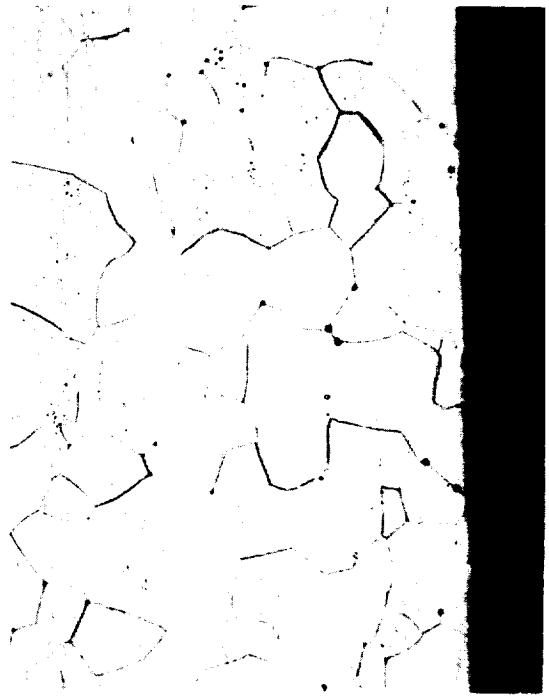

(b) After biaxial creep testing for 100 hours at 1699K (2600° F) and $3.00X10^7$ N/m^2 (4350 psi).

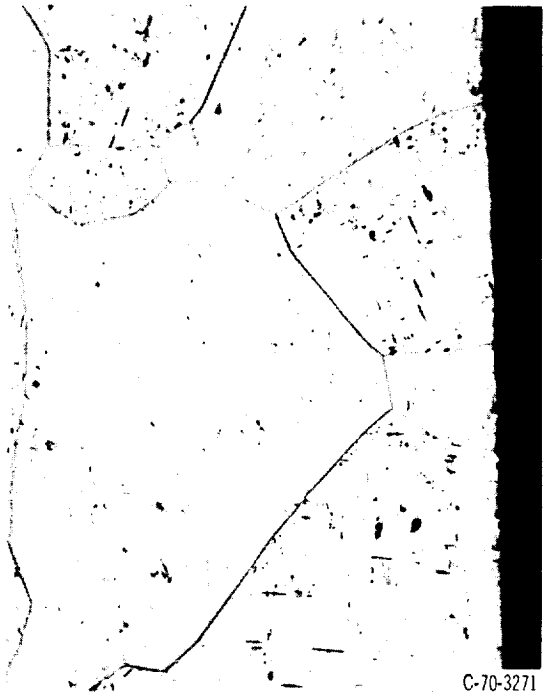

(c) After biaxial creep testing for 340 hours at 1922K (3000° F) and $8.76X10^6$ N/m^2 (1270 psi).

Figure 9. - Microstructure of T-111 after heat treating for 1 hour at 1922 K (3000° F) and biaxial creep testing. Etchant, 3 parts HNO_3, 1 part HF. X250.

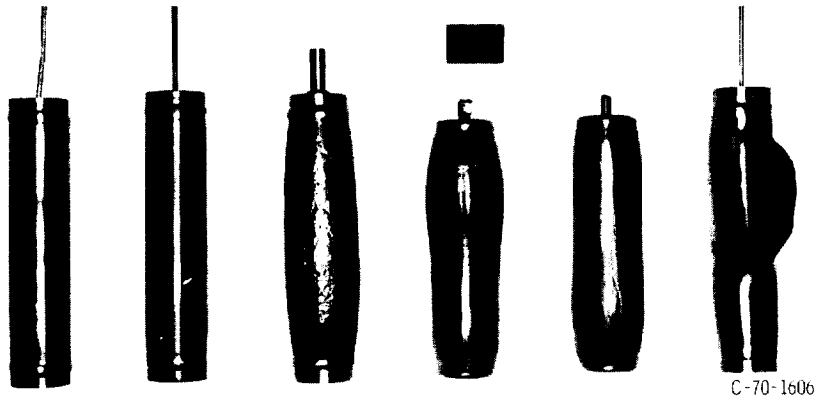

Figure 10. - Creep-tested tube specimens.